



## Spectral Investigation of Yb<sup>3+</sup>/Ho<sup>3+</sup>/Tm<sup>3+</sup>:Y<sub>2</sub>Si<sub>2</sub>O<sub>7</sub> Upconverting Nanophosphors for the Usage of Temperature Sensing

Murat Erdem<sup>1\*</sup> , Kadir Esmer<sup>1</sup> , and Gonul Eryurek<sup>2</sup> 

<sup>1</sup>Marmara University, Physics Department, Istanbul, 34722, Turkey

<sup>2</sup>Istanbul Technical University, Physics Engineering Department, Istanbul, 34722, Turkey

**Abstract:** Rare earth (Yb<sup>3+</sup>, Ho<sup>3+</sup>, Tm<sup>3+</sup>) yttrium disilicate phosphors were produced by sol-gel technique and heated at 1050 °C temperature. The sizes of the phosphors vary between 20-30 nm according to the images obtained from the Transmission Electron Microscope. The up-conversion (UC) emissions of the nanopowders were measured in the range of 500–900 nm wavelength under 950 nm laser excitation. A linear increase with power was observed in the emission intensity ratio depending on the laser excitation power. Using the FIR technique, the phosphor's temperature was determined by the heating effect caused by the laser pump power. Due to the change in intensity ratio versus temperature, the temperature sensitivity at 428 K was calculated as 0.781x10<sup>-2</sup>K<sup>-1</sup> and it was suggested that it can be used as a promising temperature sensor probe in photonic devices.

**Keywords:** Nanophosphors; Sol-gel; Up-conversion; Temperature sensing.

**Submitted:** August 08, 2022. **Accepted:** November 07, 2022.

**Cite this:** Erdem M, Esmer K, Eryurek G. Spectral investigation of Yb<sup>3+</sup>/Ho<sup>3+</sup>/Tm<sup>3+</sup>:Y<sub>2</sub>Si<sub>2</sub>O<sub>7</sub> upconverting nanophosphors for the usage of temperature sensing. Journal of the Turkish Chemical Society, Section A: Chemistry. 2023;10(1):55–62.

**DOI:** <https://doi.org/10.18596/jotcsa.1159026>.

**\*Corresponding author. E-mail:** [merdem@marmara.edu.tr](mailto:merdem@marmara.edu.tr).

### 1. INTRODUCTION

The optical temperature sensing of luminescent materials, which detects temperature changes precisely at small spatial resolution in inaccessible environments, has attracted great interest recently, especially concerning their high-temperature sensitivity (1-6). Luminescent thermography-based temperature sensing is an alternative method, which stands out with its non-contact measurements in many areas that traditional thermometers cannot reach, such as high-voltage power plants, microfluidics, bio-objects, and small-sized circuits below 10 μm (7,8).

The laser excitation power induces heat, which increases the temperature of the rare earth (RE) doped phosphors. Therefore, the emission intensities of RE<sup>3+</sup> ions become sensitive to temperature change. Consequently, the sensitive effect of excitation power on emission intensity can

lead to the calculation of the temperature of phosphors using the Boltzmann electron distribution between the nearest neighbor energy levels (9). As the difference in nearest energy levels of some RE<sup>3+</sup> ions varies between about 200 cm<sup>-1</sup> and 2000 cm<sup>-1</sup> (10), this benefits the development of temperature-sensitive phosphors for optical thermometers.

The optical thermometer properties of RE<sup>3+</sup>: Yb<sup>3+</sup>/Ho<sup>3+</sup> doped phosphors are limited to a few studies. For example, the sensor sensitivities are 0.0053 K<sup>-1</sup> at 93 K for Yb<sup>3+</sup>/Ho<sup>3+</sup>:BaCaTiO<sub>3</sub>, 0.0077 K<sup>-1</sup> at 366 K for Yb<sup>3+</sup>/Ho<sup>3+</sup>: Pb(MgNb)O<sub>3</sub>PbTiO<sub>3</sub>, and 0.005 K<sup>-1</sup> at 923 K for Yb<sup>3+</sup>/Ho<sup>3+</sup>: CaWO<sub>4</sub>, respectively (11-13). The primary goal in the field of optical thermometry is to manufacture the sensor with the highest sensitivity. Therefore, the selection of suitable host materials for the high solubility of RE ions may provide a significant advantage in luminescence properties for the development of optical temperature sensing. Among the many main

lattices, yttrium disilicate ( $\text{Y}_2\text{Si}_2\text{O}_7$ ) activated by  $\text{RE}^{3+}$  ions, either by the upconversion or by direct excitation, has attracted attention due to white light generation in practical uses for LED applications (14-19). Unlike these studies, it has been proposed to use  $\text{Y}_2\text{Si}_2\text{O}_7$  nano phosphors doped with  $\text{Yb}^{3+}/\text{Ho}^{3+}/\text{Tm}^{3+}$  ions as temperature sensing probes from the up-conversion spectral intensity ratios depending on the laser excitation power.

## 2. MATERIALS AND METHODS

The chemicals with a purity of 99.9%, which were bought from Sigma-Aldrich used to synthesize nanocrystalline  $\alpha\text{-Y}_2\text{Si}_2\text{O}_7$  doped with  $\text{RE}^{3+}$ . To obtain desired phosphor powders tetraethyl orthosilicate, yttrium(III) hexahydrate nitrate, ytterbium(III) nitrate pentahydrate, holmium(III) nitrate pentahydrate, thulium(III) nitrate were employed as precursors with a proper stoichiometry by sol-gel technique. Preparation method of  $\text{RE}^{3+}$  doped  $\text{Y}_2\text{Si}_2\text{O}_7$  as detailed in our previous work (20).

In the set of YSYHT compositions,  $\text{Yb}^{3+}$  and  $\text{Tm}^{3+}$  molar ratios were kept at 2.0 and 0.5 respectively.  $\text{Ho}^{3+}$  molar percentage ratios were also increased from 0.5 to 1.5 with the step of 0.5. Thus, three different compositions of YSYHT were obtained and labeled as YSYHT1, YSYHT2, and YSYHT3. All prepared compounds were heated at 1050 °C for 12 h.

The structural and morphological properties of the powders were investigated by Bruker D2 Phaser model X-ray diffractometer, JEOL-JEM-2100 model High resolution-Transmission Emission Microscope,

and FEI Inc. Inspect S50 model Scanning Electron Microscope. Energy dispersive X-ray measurements were taken using an EDAX Inc.-Octane Prime spectrometer to analyze the elements in the compound. The selected field diffraction (SAED) pattern was also taken to evaluate the crystallinity of the sample.

A UV-Vis spectrophotometer (Perkin-Elmer Lambda 35) was used to reveal absorption lines from diffuse reflectance spectra of  $\text{RE}^{3+}$  ions in the spectral wavelength range between 400 and 1050 nm at room temperature. A laser diode source with a 950 nm wavelength (Laser Drive Inc. LDI-820) was utilized to investigate the UC photoluminescence of the phosphors. The McPearson Inc. Model 2051 Monochromator with a PMT (Hamamatsu R1387) detector was used to measure the spectral outputs of the phosphors. To prevent light scattered from the material in different directions from entering the monochromator, a short-wavelength filter (850 nm) was placed prior to the monochromator. The measured data were processed by an EG&G Model 5210 lock-in amplifier and saved to the computer using the Labview program.

## 3. RESULTS AND DISCUSSION

### 3.1. Structural Studies

Figure 1 demonstrates the XRD patterns of YSYHT nanopowders. The figures show that most of the diffraction peak locations for three powders show good agreement with the JCPDS: 38-0223 card data of  $\alpha\text{-Y}_2\text{Si}_2\text{O}_7$ . In addition, no other phase was detected apart from the  $\alpha\text{-Y}_2\text{Si}_2\text{O}_7$  phase seen in XRD measurements of all powders.

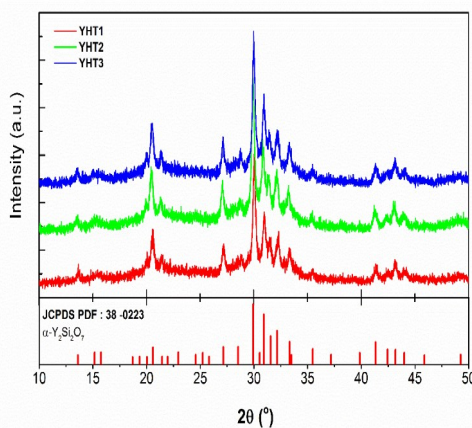


**Figure 1:** XRD graphs of  $\text{Yb}^{3+}$ ,  $\text{Ho}^{3+}$ , and  $\text{Tm}^{3+}$  doped  $\text{Y}_2\text{Si}_2\text{O}_7$  samples annealed at 1050 °C.

The electron microscope images, elemental analysis (EDAX), and selected area diffraction pattern (SAED) of YSHYT nanopowders are presented in Figure 2. As seen in SEM and TEM images of the triple rare-earth-doped  $\alpha\text{-Y}_2\text{Si}_2\text{O}_7$  nanoparticles, the

samples consist of nearly spherical nanoparticles ranging in size from about 20 to 40 nm. In addition, the peaks obtained from the EDAX spectrum of the nanoparticles given in Figure 2 show the elemental presence of Y, Si, O<sub>2</sub>, Yb, Ho, and Tm in the phosphorus material.

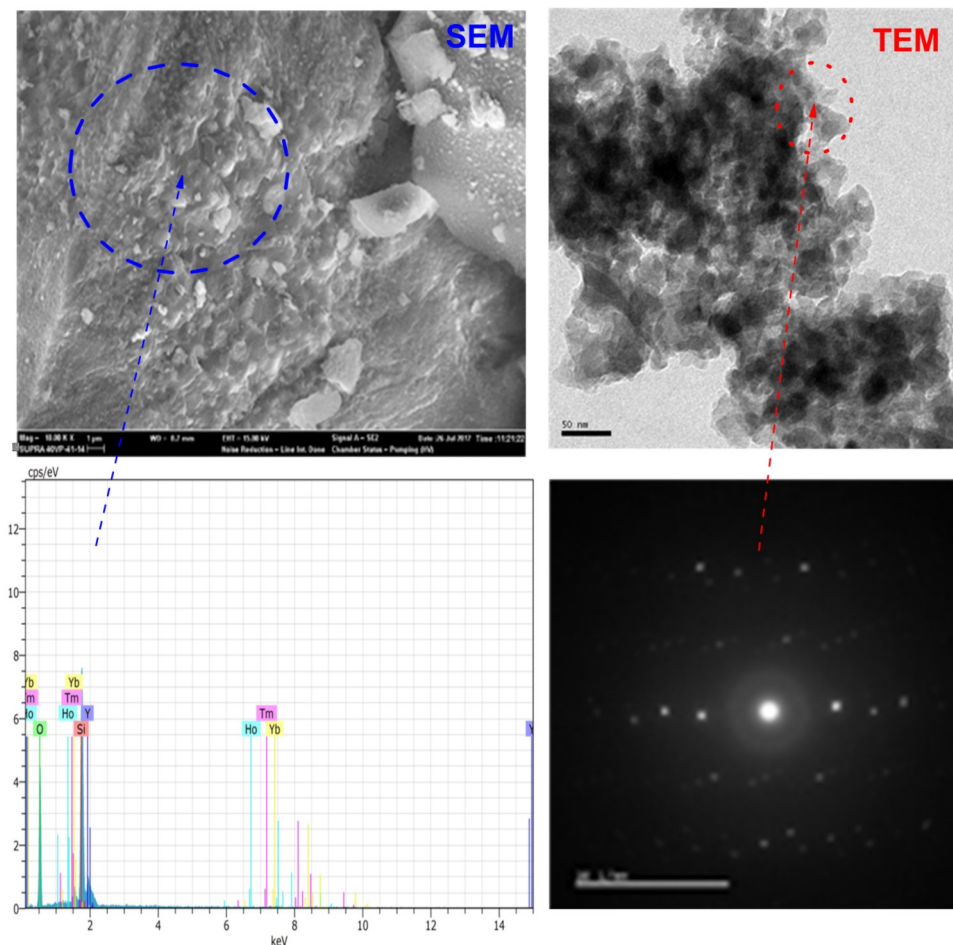


**Figure 2:** Electron microscope images, EDAX spectrum, and SAED pattern of  $\text{Yb}^{3+}/\text{Ho}^{3+} / \text{Tm}^{3+}$  doped  $\alpha\text{-Y}_2\text{Si}_2\text{O}_7$  (YSYHT2).

### 3.2. Spectral Studies

#### 3.2.1. Diffuse Reflectance Spectra

Figure 1 shows the diffuse reflection spectra of the  $\text{Yb}:\text{Ho}:\text{Tm}$  doped  $\alpha\text{-Y}_2\text{Si}_2\text{O}_7$  samples in the 400 – 1050 nm range. Of the eleven absorption bands that appear, six absorption bands correspond to different excited states of  $\text{Ho}^{3+}$  ions from the  $^5\text{I}_8$  ground state. Three absorption bands are corresponding to the different excited states of  $\text{Tm}^{3+}$  ions from the  $^4\text{I}_{15/2}$  ground state transitions. In addition, only one  $\text{Yb}^{3+}$  absorption corresponds to the  $^2\text{F}_{7/2} \rightarrow ^2\text{F}_{5/2}$  transition.

#### 3.2.2. Upconversion luminescence of the samples

Figure 4 demonstrates the UC emission spectra of the elements in the range of 500-850 nm under 950 nm excitation. The green emissions around 525 and 547 nm were ascribed to the  $^5\text{F}_4 \rightarrow ^5\text{I}_8$  and  $^5\text{S}_2 \rightarrow ^5\text{I}_8$

transitions of the  $\text{Ho}^{3+}$  ions, respectively. The red emission around 660 nm was attributed to the  $^5\text{F}_5 \rightarrow ^5\text{I}_8$  transition of  $\text{Ho}^{3+}$  ions and  $^3\text{F}_{2,3} \rightarrow ^3\text{H}_6$  transition of  $\text{Tm}^{3+}$  ions. The turquoise blue (492 nm) and infrared emission (790 nm) were also attributed to the  $^1\text{G}_4 \rightarrow ^3\text{H}_6$  ( $\text{Tm}^{3+}$ ) and  $^3\text{H}_4 \rightarrow ^3\text{H}_6$  ( $\text{Tm}^{3+}$ ) transitions, respectively.

Figure 5 indicates the UC emission spectra depending on the laser pump power. The calculated slope values of triple doped  $\alpha\text{-Y}_2\text{Si}_2\text{O}_7$  nanoparticles were found to be 1.4, 2.2, and 3.1 for red, green, and blue emissions, respectively. According to slope values, while the red (660 nm) and green (525 nm) emissions are taking place via a two-photon absorption process, the turquoise blue emission (492 nm) is based on three-photon absorption.

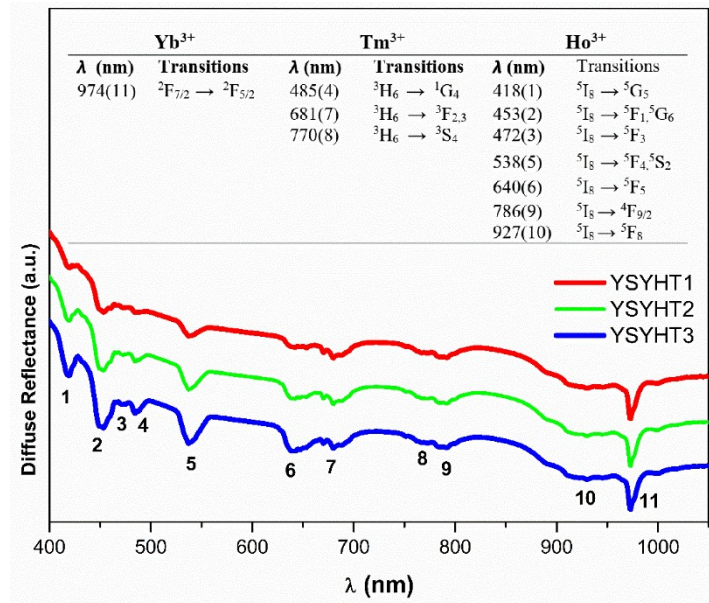


Figure 3: Diffuse Reflectance spectra of YSYHT samples.

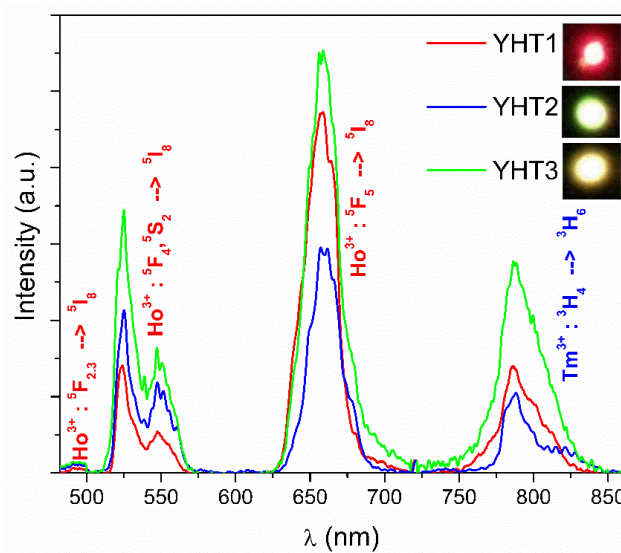
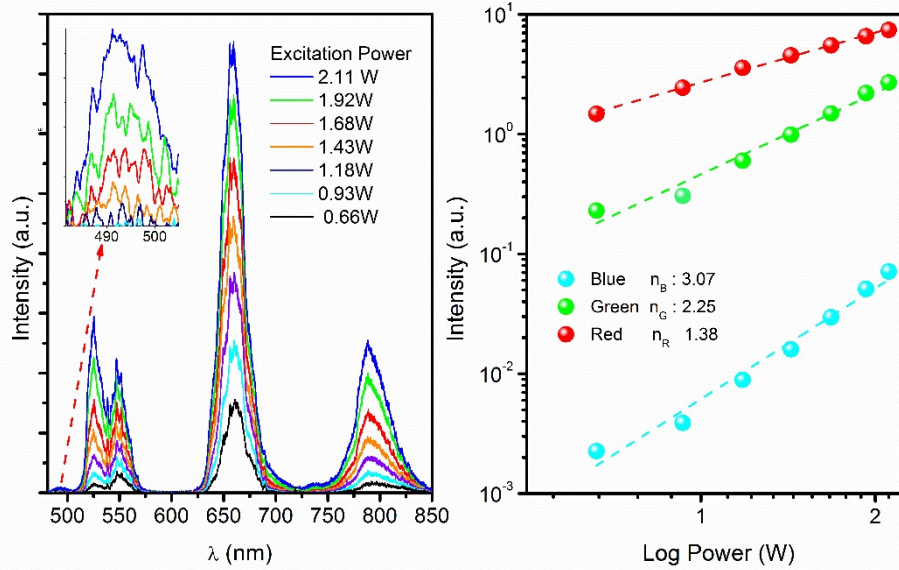


Figure 4: UC luminescence spectra of YSYHT samples.

The energy transfer from the Yb<sup>3+</sup> ions to the Ho<sup>3+</sup> and Tm<sup>3+</sup> ions can efficiently occur to populate the high excited levels of those due to energy match among those. As indicated in Figure 6, the following points can be made (21-24):

- i. The energy transfer from the Yb<sup>3+</sup> ions to the Ho<sup>3+</sup> ions occurs by the process of <sup>5</sup>I<sub>8</sub> (Ho<sup>3+</sup>) + <sup>2</sup>F<sub>5/2</sub> (Yb<sup>3+</sup>) → <sup>5</sup>I<sub>6</sub> (Ho<sup>3+</sup>) + <sup>2</sup>F<sub>7/2</sub> (Yb<sup>3+</sup>). And it may be responsible for the increase of the population of <sup>5</sup>I<sub>6</sub> (Ho<sup>3+</sup>) level.
- ii. The <sup>5</sup>I<sub>6</sub> level of Ho<sup>3+</sup> is populated with the probable ways as follows: <sup>5</sup>I<sub>6</sub> (Ho<sup>3+</sup>) + <sup>2</sup>F<sub>5/2</sub> (Yb<sup>3+</sup>) → <sup>5</sup>F<sub>4,5</sub>S<sub>2</sub> (Ho<sup>3+</sup>) + <sup>2</sup>F<sub>7/2</sub> energy transfer or <sup>5</sup>I<sub>6</sub> (Ho<sup>3+</sup>) + a photon (950nm) → <sup>5</sup>F<sub>4,5</sub>S<sub>2</sub> (Ho<sup>3+</sup>). These processes fill the <sup>5</sup>F<sub>4/5</sub>S<sub>2</sub> level of Ho<sup>3+</sup>, and then the <sup>5</sup>F<sub>4/5</sub>S<sub>2</sub> level relaxes to the <sup>5</sup>I<sub>8</sub> (Ho<sup>3+</sup>) level. Consequently, these processes cause the green emission at 525 and 547 nm corresponding to <sup>5</sup>F<sub>4</sub>→<sup>5</sup>I<sub>8</sub>, and <sup>5</sup>S<sub>2</sub>→<sup>5</sup>I<sub>8</sub> transitions, respectively.
- iii. In the red emission process, with the help of non-radiative transitions, both the transitions from the <sup>5</sup>F<sub>4/5</sub>S<sub>2</sub> levels populate the <sup>5</sup>F<sub>5</sub> level, and the transitions from the <sup>5</sup>I<sub>6</sub> level to the <sup>5</sup>I<sub>7</sub> take place. Then the <sup>5</sup>F<sub>5</sub> level can be populated through the <sup>5</sup>I<sub>7</sub> → <sup>5</sup>F<sub>5</sub> transition via the energy transfer process from <sup>5</sup>I<sub>7</sub> (Ho<sup>3+</sup>) + <sup>2</sup>F<sub>5/2</sub> (Yb<sup>3+</sup>) → <sup>5</sup>F<sub>5</sub> (Ho<sup>3+</sup>) + <sup>5</sup>F<sub>7/2</sub> (Yb<sup>3+</sup>) transition. Finally, the red emission at 660 nm comes true via <sup>5</sup>F<sub>5</sub> → <sup>5</sup>I<sub>8</sub> transition.



**Figure 5:** UC luminescence intensity vs. Excitation power for the YSYHT2 sample.

iv. In the blue emission (492 nm) process, the  ${}^5F_{2,3}$  excited energy level of the  $\text{Ho}^{3+}$  ion can be populated by the energy transfer from the  $\text{Yb}^{3+}$  ions in the ground state via three-photon processes. This process is as follows:  ${}^5I_5 (\text{Ho}^{3+}) + {}^2F_{5/2} (\text{Yb}^{3+}) \rightarrow {}^5F_{2,3} (\text{Ho}^{3+}) + {}^5F_{7/2} (\text{Yb}^{3+})$  energy transfer.

v. Consequently,  $\text{Tm}^{3+}$  ions at level  ${}^3H_6$  can fill the  ${}^1G_4$  level via energy transfer from  $\text{Yb}^{3+}$  to the  $\text{Tm}^{3+}$  ions. Then the  ${}^1G_4 (\text{Tm}^{3+}) \rightarrow {}^3F_4 (\text{Tm}^{3+})$  transition cause the red emission (651 nm). In addition, the  ${}^3F_{2,3} \rightarrow {}^3H_4$  transition occurs thanks to non-radiative processes. Thus, the transition from the  ${}^3H_4$  level to the  ${}^3H_6 (\text{Tm}^{3+})$  level produces infrared emission at 790 nm.

The UC spectral profiles of YSYHT phosphors at different power values of 950 nm excitation are additionally shown in Figure 7a. The UC emission intensity ratio is found from the intensity ratio of the  ${}^5F_4 \rightarrow {}^5I_8$  (525 nm) and  ${}^5S_2 \rightarrow {}^5I_8$  (547 nm) transitions of the  $\text{Ho}^{3+}$  ion.

The energy difference ( $\Delta E_s$ ) provided by these two transitions in the spectra was calculated to be  $766.03 \text{ cm}^{-1}$ . As seen from Figure 7a, the UC emission intensity ratio of these two close levels indicates a linear change with increasing the pump power. Therefore, the fluorescence intensity ratio (FIR) (9,25,26), on which the Boltzmann distribution of electrons is based, is used to determine the temperature-sensitive effect on the emission intensity.

The intensity ratio ( $I_R$ ) and sensitivity are functions of temperature and are given by the following equations:

$$I_R = \frac{I_2}{I_1} = A \exp\left(\frac{-\Delta E}{k_B T}\right) \quad (1)$$

$$\text{Sensitivity} = \frac{dI_R}{dT} = A \exp\left(\frac{-\Delta E}{k_B T}\right) \times \left(\frac{\Delta E}{k_B T^2}\right) \quad (2)$$

where, A is a constant that includes the frequencies of emissions, degeneration factors, and cross-sections of the emissions.  $\Delta E$  is the energy difference among the nearest two levels, and  $k_B$  is the Boltzmann's constant.

In the FIR technique, each FIR value is represented by a specific temperature (27-29). The increase in host temperature occurs with the increase of heat-inducing laser pump power. Therefore, the intensities of  $\text{RE}^{3+}$  ions' emissions become sensitive to temperature change. Now, let's consider this at low pump power (0.66 W) at room temperature. And if the spectral energy difference ( $\Delta E_s$ ) was used instead of the energy difference expressed in Equation (1), the calculated value of constant A is found as 17.615. Then the temperature of powders correlating with different intensity ratio values of the  ${}^5F_4 \rightarrow {}^5I_8$  and  ${}^5S_2 \rightarrow {}^5I_8$  transitions at different pump powers can easily be calculated using Eq. (3) which is provided in Eq. (1).

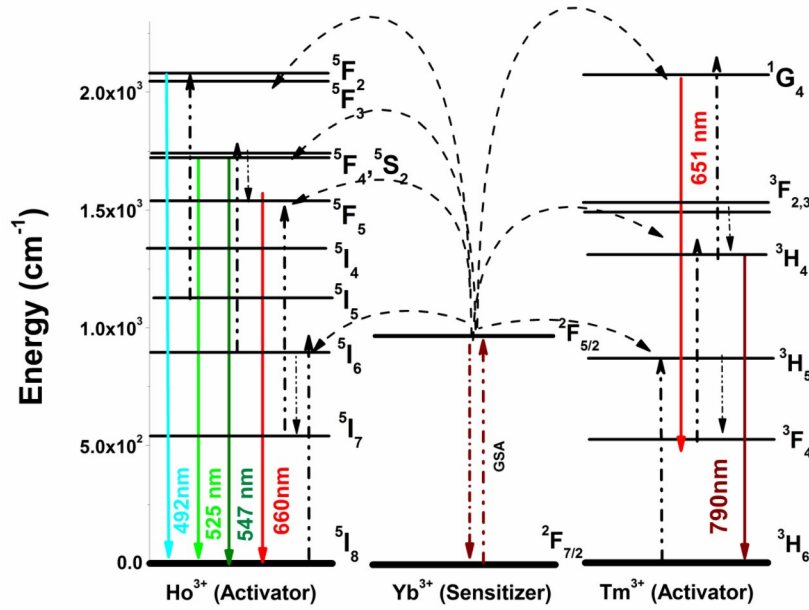


Figure 6: Possible energy transitions for Yb<sup>3+</sup>, Ho<sup>3+</sup>, and Tm<sup>3+</sup> ions in YSYHT powders.

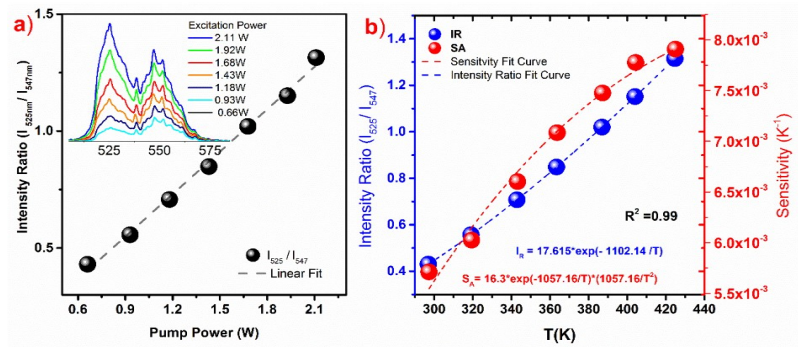


Figure 7: a) Intensity ratio of emission peaks due to laser pump power. b) Temperature sensing in terms of power heating relationship.

$$T = \left[ \frac{1}{\ln A - \ln(I_R)} \right] \frac{\Delta E}{k} \quad (3)$$

Thus, the temperatures corresponding to the different intensity ratios and the sensitivity calculated using Eq. (2) are shown in Figure 7b. The maximum sensitivity with a value of  $0.781 \times 10^{-2} \text{ K}^{-1}$  at 428 K was calculated from the fitting sensitivity curve's maximum value. When compared with the literature, this sensitivity value was found to be compatible with the sensitivity values of some RE<sup>3+</sup> doped phosphorus materials given in Table 1. Consequently, as YSYHT phosphors can convert laser excitation power into heat, these phosphors can be used in promising applications as temperature sensor probes.

#### 4. CONCLUSION

Sol-gel synthesized Yb<sup>3+</sup>:Ho<sup>3+</sup>:Tm<sup>3+</sup> doped  $\alpha$ -Y<sub>2</sub>Si<sub>2</sub>O<sub>7</sub> nano-powders indicated that most of the peaks matched well with the standard JCPDS:38-0223 card data of  $\alpha$ -Y<sub>2</sub>Si<sub>2</sub>O<sub>7</sub>. Morphology investigations with TEM microscopy showed that triple rare earth combinations mixed with  $\alpha$ -Y<sub>2</sub>Si<sub>2</sub>O<sub>7</sub> presented nearly spherical nanoparticles in size varying from 20 to 30 nm for the powders.

The diffuse reflection spectra of the powders presented reflection data matching the absorption transitions of Yb<sup>3+</sup>, Ho<sup>3+</sup> and Tm<sup>3+</sup> ions in the  $\alpha$ -Y<sub>2</sub>Si<sub>2</sub>O<sub>7</sub> samples in the 400 – 1050 nm. Up-converted blue, green, and red emissions were obtained in the visible region from Yb<sup>3+</sup>:Ho<sup>3+</sup>:Tm<sup>3+</sup> doped  $\alpha$ -Y<sub>2</sub>Si<sub>2</sub>O<sub>7</sub> nano-powders at 950 nm laser excitation. The slope values of laser power intensity revealed that the up-conversion mechanism comes true via two and three-photon absorption processes.

The UC emission intensity ratio of the  ${}^5F_4 \rightarrow {}^5I_8$  and  ${}^5S_2 \rightarrow {}^5I_8$  transitions corresponding to the  $\text{Ho}^{3+}$  ion depends on the pump power. Depending on the variation of the laser excitation power with the emission intensity ratio, the temperature range of 297-425 K corresponding to the laser excitation

power range of 0.66 – 2.11 W was calculated by the FIR technique. The maximum sensitivity value of  $7.81 \times 10^{-3} \text{ K}^{-1}$  at 428 K was determined from the fitting sensitivity curve's maximum value. Consequently,  $\text{Yb}^{3+}:\text{Ho}^{3+}:\text{Tm}^{3+}$  doped  $\alpha\text{-Y}_2\text{Si}_2\text{O}_7$  nano-phosphors can be used as promising temperature sensor probes in photonic devices.

**Table1:** Sensitivity values of some  $\text{RE}^{3+}$  doped phosphorus materials.

Materials	Temperature Range [K]	Intensity Ratio	Sensitivity [ $\text{K}^{-1}$ ]	Ref.
$\text{Yb}^{3+}/\text{Ho}^{3+}/\text{Tm}^{3+}:\text{Y}_2\text{Si}_2\text{O}_7$	290-440	$I_{525}/I_{547}$	0.0078 @ 428 K	Present work
$\text{Yb}^{3+}/\text{Ho}^{3+}:\text{Ba}_{0.77}\text{Ca}_{0.23}\text{TiO}_3$	93-300	$I_{525}/I_{547}$	0.0053 @ 93 K	(11)
$\text{Yb}^{3+}/\text{Ho}^{3+}:\text{CaWO}_4$	298-553	$I_{460}/I_{487}$	0.005 @ 923 K	(13)
$\text{Yb}^{3+}/\text{Ho}^{3+}:\text{TeO}_2\text{-ZnO-BaO}$	303-503	$I_{660}/I_{547}$	0.0073 @ 503 K	(22)
$\text{Yb}^{3+}/\text{Ho}^{3+}:\text{PSN-PMN-PT}$	173-493	$I_{665}/I_{554}$	0.0022 @ 93 K	(30)
$\text{Yb}^{3+}/\text{Ho}^{3+}:\text{KLa}(\text{MoO}_4)_2$	293-473	$I_{651}/I_{546}$	0.0356 @ 503 K	(31)
$\text{Yb}^{3+}/\text{Ho}^{3+}:(\text{Y}_{0.88},\text{La}_{0.09},\text{Zr}_{0.03})_2\text{O}_3$	293-563	$I_{667}/I_{549}$	0.0071 @ 563K	(32)

## 5. CONFLICT OF INTEREST

There are no conflicts that need to be reported.

## 6. ACKNOWLEDGMENTS

The study was carried out with the support of the Marmara University Scientific Research Projects Unit, project number FEN-B-150513-0170. We thank Prof. Dr. Baldassare Di Bartolo for the photoluminescent measurements performed in the Spectroscopy Laboratory at Boston College.

## 7. REFERENCES

- Marciniak L, Waszniewska K, Bednarkiewicz A, Hreniak D, Strek W. Sensitivity of a Nanocrystalline Luminescent Thermometer in High and Low Excitation Density Regimes. *J Phys Chem C* [Internet]. 2016 Apr 28 [cited 2022 Nov 27];120(16):8877–82. Available from: [<URL>](#)
- Marciniak L, Bednarkiewicz A, Kowalska D, Strek W. A new generation of highly sensitive luminescent thermometers operating in the optical window of biological tissues. *J Mater Chem C* [Internet]. 2016 [cited 2022 Nov 27];4(24):5559–63. Available from: [<URL>](#)
- Balabhadra S, Debasu ML, Brites CDS, Nunes LAO, Malta OL, Rocha J, et al. Boosting the sensitivity of Nd<sup>3+</sup>-based luminescent nanothermometers. *Nanoscale* [Internet]. 2015 [cited 2022 Nov 27];7(41):17261–7. Available from: [<URL>](#)
- Du P, Tang J, Li W, Luo L. Exploiting the diverse photoluminescence behaviors of  $\text{NaLuF}_4:\text{xEu}^{3+}$  nanoparticles and g-C<sub>3</sub>N<sub>4</sub> to realize versatile applications in white light-emitting diode and optical thermometer. *Chem Eng J* [Internet]. 2021 Feb [cited 2022 Nov 27];406:127165. Available from: [<URL>](#)
- Doğan A, Erdem M. Investigation of the optical temperature sensing properties of up-converting  $\text{TeO}_2\text{-ZnO-BaO}$  activated with  $\text{Yb}^{3+}/\text{Tm}^{3+}$  glasses. *Sens Actuat A: Phys* [Internet]. 2021 May [cited 2022 Nov 27];322:112645. Available from: [<URL>](#)
- Doğan A, Yıldırım SM, Erdem M, Esmer K, Eryürek G. Investigation of spectral output of  $\text{Er}^{3+}$  and  $\text{Yb}^{3+}/\text{Er}^{3+}$  doped  $\text{TeO}_2\text{-ZnO-BaO}$  glasses for photonic applications. *New J Chem* [Internet]. 2021 [cited 2022 Nov 27];45(8):3790–9. Available from: [<URL>](#)
- Liu X, Chen Y, Shang F, Chen G, Xu J. Wide-range thermometry and up-conversion luminescence of  $\text{Ca}_5(\text{PO}_4)_3\text{F}:\text{Yb}^{3+}/\text{Er}^{3+}$  transparent glass ceramics. *J Mater Sci: Mater Electron* [Internet]. 2019 Mar [cited 2022 Nov 27];30(6):5718–25. Available from: [<URL>](#)
- Fischer LH, Harms GS, Wolfbeis OS. Upconverting Nanoparticles for Nanoscale Thermometry. *Angew Chem Int Ed* [Internet]. 2011 May 9 [cited 2022 Nov 27];50(20):4546–51. Available from: [<URL>](#)
- Wade SA, Collins SF, Baxter GW. Fluorescence intensity ratio technique for optical fiber point temperature sensing. *J Appl Phys* [Internet]. 2003 [cited 2022 Nov 27];94(8):4743. Available from: [<URL>](#)
- Lei R, Luo X, Yuan Z, Wang H, Huang F, Deng D, et al. Ultrahigh-sensitive optical temperature sensing in  $\text{Pr}^{3+}:\text{Y}_2\text{Ti}_2\text{O}_7$  based on diverse thermal response from trap emission and  $\text{Pr}^{3+}$  red luminescence. *J Lumin* [Internet]. 2019 Jan [cited 2022 Nov 27];205:440–5. Available from: [<URL>](#)
- Du P, Luo L, Yu JS. Low-temperature thermometry based on upconversion emission of  $\text{Ho}/\text{Yb}$ -codoped  $\text{Ba}_{0.77}\text{Ca}_{0.23}\text{TiO}_3$  ceramics. *J Alloy Comp* [Internet]. 2015 May [cited 2022 Nov 27];632:73–7. Available from: [<URL>](#)

12. Liu Z, Jiang G, Wang R, Chai C, Zheng L, Zhang Z, et al. Temperature and concentration effects on upconversion photoluminescence properties of  $\text{Ho}^{3+}$  and  $\text{Yb}^{3+}$  codoped  $0.67\text{Pb}(\text{Mg}_{1/3}\text{Nb}_{2/3})\text{O}_3-0.33\text{PbTiO}_3$  multifunctional ceramics. *Ceram Int* [Internet]. 2016 Jul [cited 2022 Nov 27];42(9):11309–13. Available from: [<URL>](#)
13. Xu W, Zhao H, Li Y, Zheng L, Zhang Z, Cao W. Optical temperature sensing through the upconversion luminescence from  $\text{Ho}^{3+}/\text{Yb}^{3+}$  codoped  $\text{CaWO}_4$ . *Sens Actuat B: Chem* [Internet]. 2013 Nov [cited 2022 Nov 27];188:1096–100. Available from: [<URL>](#)
14. Marciniak L, Hreniak D, Strek W, Piccinelli F, Spgehini A, Bettinelli M, et al. Spectroscopic and structural properties of polycrystalline  $\text{Y}_2\text{Si}_2\text{O}_7$  doped with  $\text{Er}^{3+}$ . *J Lumin* [Internet]. 2016 Feb [cited 2022 Nov 27];170:614–8. Available from: [<URL>](#)
15. Sokolnicki J. Rare earths (Ce, Eu, Tb) doped  $\text{Y}_2\text{Si}_2\text{O}_7$  phosphors for white LED. *J Lumin* [Internet]. 2013 Feb [cited 2022 Nov 27];134:600–6. Available from: [<URL>](#)
16. Erdem M, Sitt B. Up conversion based white light emission from sol-gel derived  $\alpha\text{-Y}_2\text{Si}_2\text{O}_7$  nanoparticles activated with  $\text{Yb}^{3+}$ ,  $\text{Er}^{3+}$  ions. *Optical Materials* [Internet]. 2015 Aug [cited 2022 Nov 27];46:260–4. Available from: [<URL>](#)
17. Erdem M, Tabanlı S, Eryurek G, Samur R, Di Bartolo B. Crystalline phase effect on the up-conversion processes and white emission of  $\text{Yb}^{3+}/\text{Er}^{3+}/\text{Tm}^{3+}:\text{Y}_2\text{Si}_2\text{O}_7$  nanocrystals. *Dalton Trans* [Internet]. 2019 [cited 2022 Nov 27];48(19):6464–72. Available from: [<URL>](#)
18. Tomala R, Hreniak D, Strek W. Laser induced broadband white emission of  $\text{Y}_2\text{Si}_2\text{O}_7$  nanocrystals. *J Rare Earths* [Internet]. 2019 Nov [cited 2022 Nov 27];37(11):1196–9. Available from: [<URL>](#)
19. Rakov N.  $\text{Tm}^{3+}, \text{Yb}^{3+}:\text{Y}_2\text{SiO}_5$  up-conversion phosphors: Exploration of temperature sensing performance by monitoring the luminescence emission. *Physica B: Cond Mat* [Internet]. 2022 Mar [cited 2022 Nov 27];628:413572. Available from: [<URL>](#)
20. Erdem M, Özen G, Tav C. Crystallization behaviour of neodymium doped yttrium silicate nanophosphors. *Journal of the Eur Ceram Soc* [Internet]. 2011 Nov [cited 2022 Nov 27];31(14):2629–31. Available from: [<URL>](#)
21. Jiang C, Xu W. Theoretical Model of  $\text{Yb}^{3+}/\text{Er}^{3+}/\text{Tm}^{3+}$ -Codoped System for White Light Generation. *J Display Technol* [Internet]. 2009 Aug [cited 2022 Nov 27];5(8):312–8. Available from: [<URL>](#)
22. Doğan A, Erdem M, Esmer K, Eryürek G. Upconversion luminescence and temperature sensing characteristics of  $\text{Ho}^{3+}/\text{Yb}^{3+}$  co-doped tellurite glasses. *J Non-Cryst Sol* [Internet]. 2021 Nov [cited 2022 Nov 27];571:121055. Available from: [<URL>](#)
23. Tavares MCP, da Costa EB, Bueno LA, Gouveia-Neto AS. White phosphor using  $\text{Yb}^{3+}$ -sensitized  $\text{Er}^{3+}$ - and  $\text{Tm}^{3+}$ -doped sol-gel derived lead-fluorosilicate transparent glass ceramic excited at 980 nm. *Opt Mater* [Internet]. 2018 Jan [cited 2022 Nov 27];75:733–8. Available from: [<URL>](#)
24. Pandey A, Rai VK. Colour emission tunability in  $\text{Ho}^{3+}-\text{Tm}^{3+}-\text{Yb}^{3+}$  co-doped  $\text{Y}_2\text{O}_3$  upconverted phosphor. *Appl Phys B* [Internet]. 2012 Dec [cited 2022 Nov 27];109(4):611–6. Available from: [<URL>](#)
25. Wade SA. Temperature measurement using rare earth doped fibre fluorescence [Internet] [PhD Thesis]. [Australia]: Victoria University; 1999. Available from: [<URL>](#)
26. Wang X, Liu Q, Bu Y, Liu CS, Liu T, Yan X. Optical temperature sensing of rare-earth ion doped phosphors. *RSC Adv* [Internet]. 2015 [cited 2022 Nov 27];5(105):86219–36. Available from: [<URL>](#)
27. Tang J, Du P, Li W, Luo L. Boosted thermometric performance in  $\text{NaGdF}_4:\text{Er}^{3+}/\text{Yb}^{3+}$  upconverting nanorods by  $\text{Fe}^{3+}$  ions doping for contactless nanothermometer based on thermally and non-thermally coupled levels. *J Lumin* [Internet]. 2020 Aug [cited 2022 Nov 27];224:117296. Available from: [<URL>](#)
28. Du P, Luo L, Park HK, Yu JS. Citric-assisted sol-gel based  $\text{Er}^{3+}/\text{Yb}^{3+}$ -codoped  $\text{Na}_{0.5}\text{Gd}_{0.5}\text{MoO}_4$ : A novel highly-efficient infrared-to-visible upconversion material for optical temperature sensors and optical heaters. *Chem Eng J* [Internet]. 2016 Dec [cited 2022 Nov 27];306:840–8. Available from: [<URL>](#)
29. Jacinto C, Vermelho MVD, Gouveia EA, de Araujo MT, Udo PT, Astrath NGC, et al. Pump-power-controlled luminescence switching in  $\text{Yb}^{3+}/\text{Tm}^{3+}$  codoped water-free low silica calcium aluminosilicate glasses. *Appl Phys Lett* [Internet]. 2007 Aug 13 [cited 2022 Nov 27];91(7):071102. Available from: [<URL>](#)
30. He A, Xi Z, Li X, Long W, Fang P, Zhang J. Temperature dependence of upconversion luminescence and sensing sensitivity of  $\text{Ho}^{3+}/\text{Yb}^{3+}$  modified PSN-PMN-PT crystals. *J Alloy Comp* [Internet]. 2019 Sep [cited 2022 Nov 27];803:450–5. Available from: [<URL>](#)
31. Zhang Y, Wang T, Liu H, Liu D, Liu Y, Fu Z. Optical temperature sensing behavior for  $\text{KLa}(\text{MoO}_4)_2:\text{Ho}^{3+}/\text{Yb}^{3+}$  phosphors based on fluorescence intensity ratios. *Optik* [Internet]. 2020 Feb [cited 2022 Nov 27];204:164100. Available from: [<URL>](#)
32. Zhou J, Chen Y, Lei R, Wang H, Zhu Q, Wang X, et al. Excellent photoluminescence and temperature sensing properties in  $\text{Ho}^{3+}/\text{Yb}^{3+}$  codoped  $(\text{Y}_{0.88}\text{La}_{0.09}\text{Zr}_{0.03})_2\text{O}_3$  transparent ceramics. *Ceramics International* [Internet]. 2019 Apr [cited 2022 Nov 27];45(6):7696–702. Available from: [<URL>](#) .